

## Supplementary Information

# **Fluorescent Nanodiamond Scintillators for Beam Diagnostics of EUV and Soft X-Ray in Photolithographic Applications**

Yuen Yung Hui,<sup>a</sup> Chen-Yu Ho,<sup>a</sup> Teng-I Yang,<sup>b</sup> Tzu-Ping Huang,<sup>c</sup> Bing-Ming Cheng,<sup>de</sup> Yin-Yu Lee,<sup>c</sup> and Huan-Cheng Chang<sup>\*afg</sup>

<sup>a</sup> *Institute of Atomic and Molecular Sciences, Academia Sinica, Taipei City 106319, Taiwan*

<sup>b</sup> *Taiwan Instrument Research Institute, National Applied Research Laboratories, Hsinchu City 300092, Taiwan*

<sup>c</sup> *National Synchrotron Radiation Research Center, Hsinchu City 300092, Taiwan*

<sup>d</sup> *Department of Medical Research, Hualien Tzu Chi Hospital, Buddhist Tzu Chi Medical Foundation, Hualien City 970, Taiwan*

<sup>e</sup> *Center for General Education, Tzu Chi University, Hualien City 970, Taiwan*

<sup>f</sup> *Department of Chemical Engineering, National Taiwan University of Science and Technology, Taipei City 106335, Taiwan*

<sup>g</sup> *Department of Chemistry, National Taiwan Normal University, Taipei City 106, Taiwan*

\* *E-mail address: [hchang@gate.sinica.edu.tw](mailto:hchang@gate.sinica.edu.tw)*

**Table S1.** Optical properties of bulk diamonds and nanodiamonds with NV centers as EUV/SXR scintillators

Property (unit)	Values (notes)	Refs.
Refractive index	1.00 (at 1.55 nm or 800 eV)	S1
	0.96 (at 13.5 nm or 91.8 eV)	
	2.41 (at 620 nm or 2.00 eV)	
Absorption coefficient (cm <sup>-1</sup> )	$1.7 \times 10^4$ (at 1.55 nm or 800 eV)	S1
	$9.2 \times 10^4$ (at 13.5 nm or 91.8 eV)	
Emission wavelength range (nm)	550 – 800	S2 – S4
Emission maximum (nm)	620	S2 – S4
Emission lifetime (ns)	17 – 20 (NV <sup>0</sup> in bulk diamond)	S5 – S8
	28 (NV <sup>0</sup> in nanodiamond)	

## References

- S1 S. Adachi, in *Optical Constants of Crystalline and Amorphous Semiconductors: Numerical Data and Graphical Information*, ed. S. Adachi, Springer US, Boston, MA, 1999, pp. 5–17.
- S2 H.-C. Lu, Y.-C. Peng, S.-L. Chou, J.-I. Lo, B.-M. Cheng and H.-C. Chang, *Angew. Chem. Int. Ed.*, 2017, **56**, 14469–14473.
- S3 H.-C. Lu, J.-I. Lo, Y.-C. Peng, S.-L. Chou, B.-M. Cheng and H.-C. Chang, *ACS Appl. Mater. Interfaces*, 2020, **12**, 3847–3853.
- S4 T.-I. Yang, Y. Y. Hui, J.-I. Lo, Y.-W. Huang, Y.-Y. Lee, B.-M. Cheng and H.-C. Chang, *Nano Lett.*, 2023, **23**, 9811–9816.
- S5 G. Liaugaudas, G. Davies, K. Suhling, R. U. A. Khan and D. J. F. Evans, *J. Phys.: Condens. Matter*, 2012, **24**, 435503.

- S6 D. Gatto Monticone, F. Quercioli, R. Mercatelli, S. Soria, S. Borini, T. Poli, M. Vannoni, E. Vittone and P. Olivero, *Phys. Rev. B*, 2013, **88**, 155201.
- S7 E. Fraczek, V. G. Savitski, M. Dale, B. G. Breeze, P. Diggle, M. Markham, A. Bennett, H. Dhillon, M. E. Newton and A. J. Kemp, *Opt. Mater. Express*, 2017, **7**, 2571–2585.
- S8 T.-I. Yang, T. Azuma, Y.-W. Huang, Y. Y. Hui, C.-T. Chiang and H.-C. Chang, *J. Chin. Chem. Soc.*, 2023, **70**, 451–459.
- S9 J. Storteboom, P. Dolan, S. Castelletto, X. Li and M. Gu, *Opt. Express*, 2015, **23**, 11327–11333.
- S10 D. F. Edwards, in *Handbook of Optical Constants of Solids*, ed. E. D. Palik, Academic Press, Boston, 1985, pp. 547–569.
- S11 D. F. Edwards and H. R. Philipp, in *Handbook of Optical Constants of Solids*, ed. E. D. Palik, Academic Press, Boston, 1985, pp. 665–673.
- S12 Y. Y. Hui, O. J. Chen, H.-H. Lin, Y.-K. Su, K. Y. Chen, C.-Y. Wang, W. W.-W. Hsiao and H.-C. Chang, *Anal. Chem.*, 2021, **93**, 7140–7147.
- S13 J.-Y. Yuh, S.-W. Lin, L.-J. Huang, H.-S. Fung, L.-L. Lee, Y.-J. Chen, C.-P. Cheng, Y.-Y. Chin and H.-J. Lin, *J. Synchrotron Rad.*, 2015, **22**, 1312–1318.

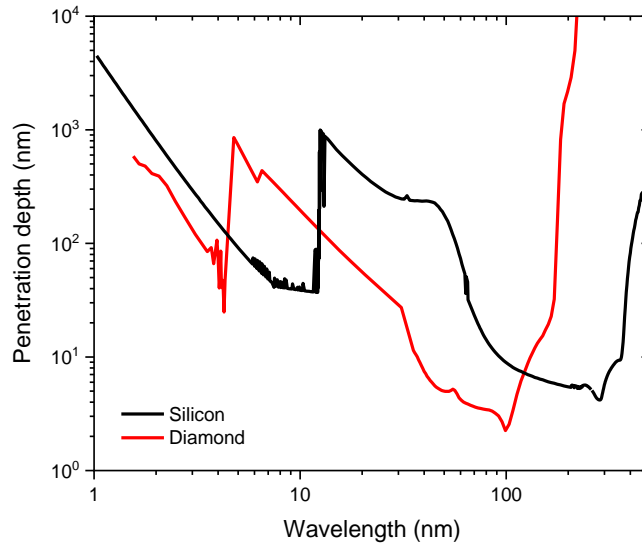


**Figure S1.** Penetration depths of EUV/SXR radiations in diamond and silicon.<sup>S10,S11</sup> The abrupt changes in the spectra result from the K-edge absorption at 284 eV (4.37 nm) of C atoms in diamond and the L2- and L3-edge absorptions at 99.2 eV (12.5 nm) of Si atoms in silicon.

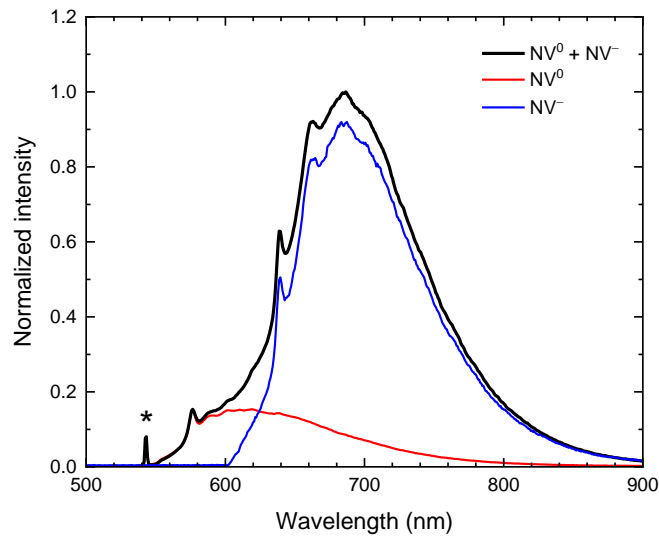


**Figure S2.** Normalized photoluminescence spectrum of an FND film excited with a continuous-wave 532-nm laser and their  $NV^0$  and  $NV^-$  components after properly scaling their spectra. The asterisk denotes the unfiltered scattered laser light at 532 nm.<sup>S8</sup>

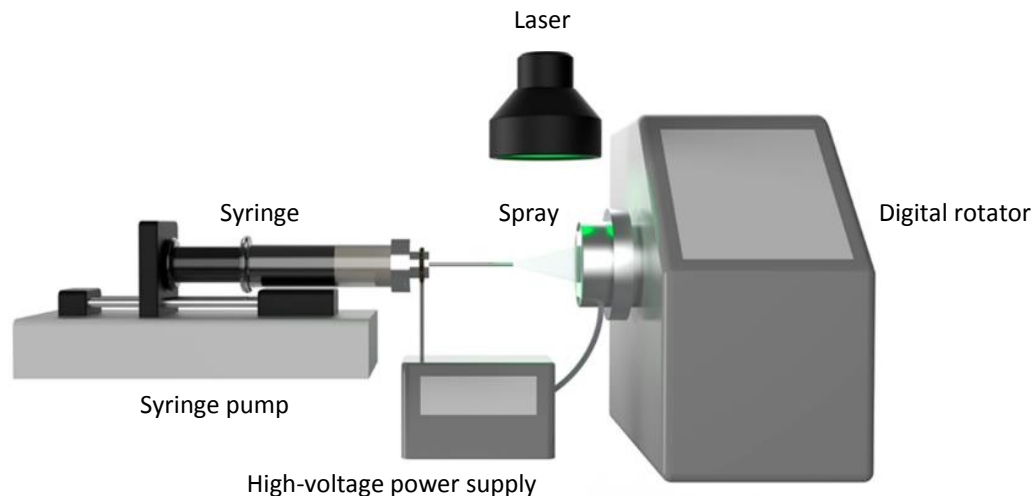


**Figure S3.** Schematic diagram of the experimental setup for electro spray deposition of an FND film on an electrically conductive plate. The wavelength of the laser is 532 nm.

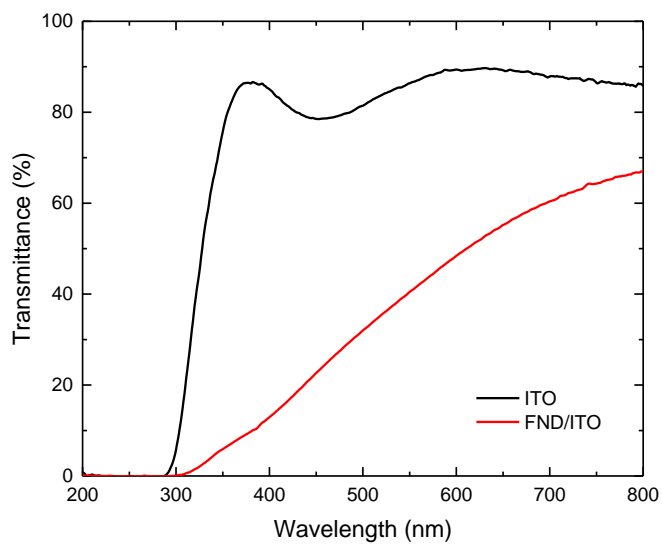


**Figure S4.** Typical transmission spectra of ITO/glass and FND-coated ITO/glass substrates. The spectra were acquired with a UV-Vis spectrophotometer (U-3310, Hitachi).

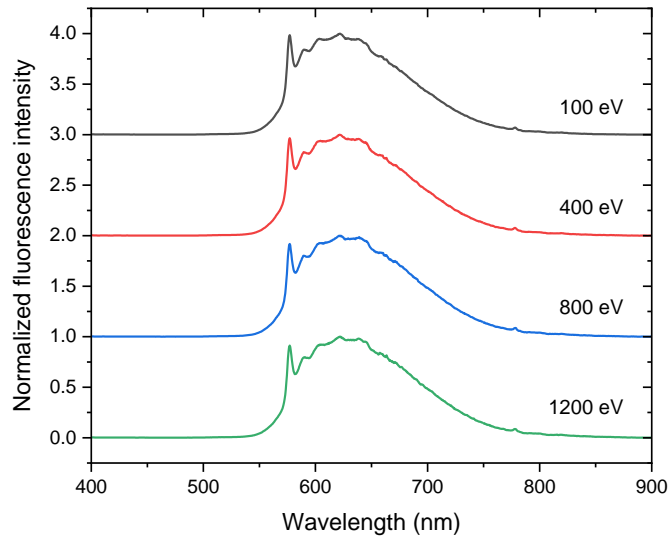


**Figure S5.** Normalized fluorescence spectra of FNDs, excited with EUV/SXR radiations of 100, 400, 800, and 1200 eV in energy. The spectra are shifted vertically for clarity. (Data taken from Ref. S3)

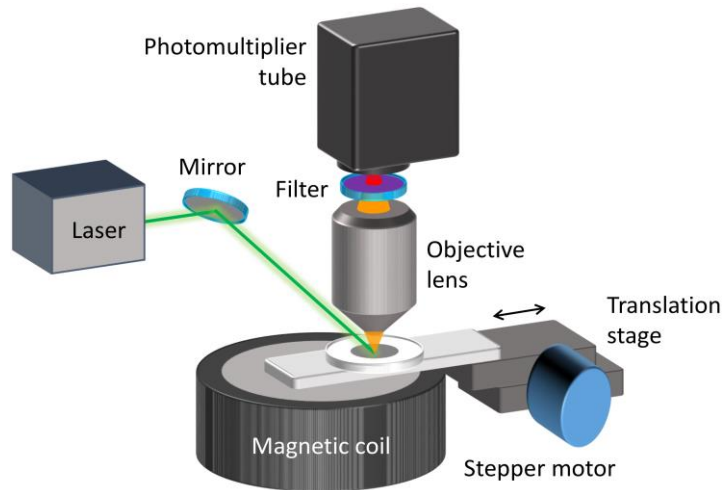


**Figure S6.** Schematic diagram of the experimental setup used to measure the radial dependence of the FND film thickness by magnetically modulated fluorescence. The sample irradiated by the laser beam is mounted on a motorized translation stage, allowing the fluorescence intensity line profile across the FND film to be obtained. The laser (532 nm in wavelength) has a beam diameter of  $\sim 0.7$  mm and a power of 10 mW.<sup>S12</sup>

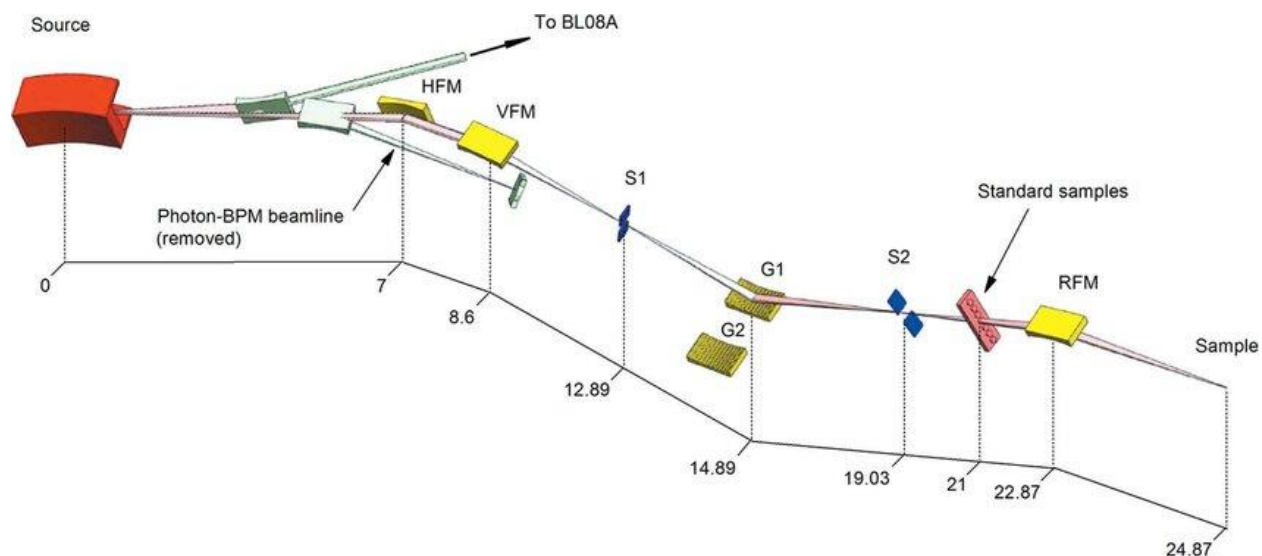


**Figure S7.** Optical layout of the BL08B beamline at NSRRC. Abbreviations are HFM: horizontal focusing mirror, VFM: vertical focusing mirror, S: slit, G: grating, RFM: refocusing mirror. The beamline has a bending magnet source. The numbers given underneath the components are distances in the units of meters. (Reproduced from Ref. S13 with permission from the International Union of Crystallography and Wiley)

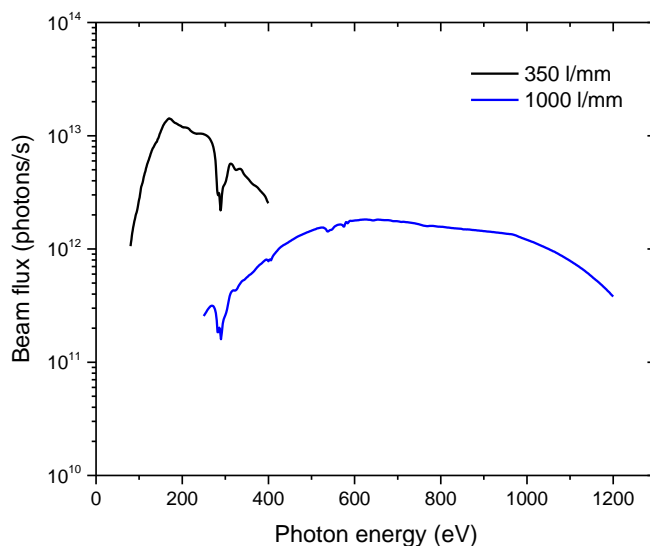


**Figure S8.** Photon energy spectra of the BL08B beamline at NSRRC. Two gratings, each having a ruling density of 350 and 1000 lines/mm, are used to disperse the radiations.

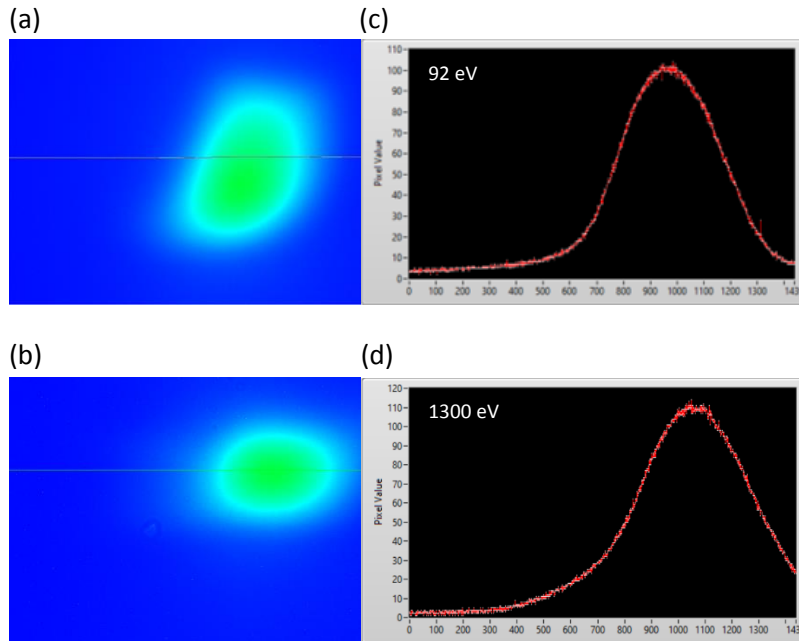


**Figure S9.** (a,b) Images and (c,d) intensity profiles of synchrotron radiations at 13.5 nm (a,c) and 0.95 nm (b,d), obtained with a lens-coupled DEUVI. The beam flux was  $7.7 \times 10^{11}$  photons/s (and  $4.5 \times 10^{10}$  photons/s), and the exposure time used to acquire the image in (a) (and b) was 0.5 s (and 2 s) with a gain of 1 dB. The pixel size of the imaging sensor on the CMOS camera was  $3.45 \mu\text{m}$ .

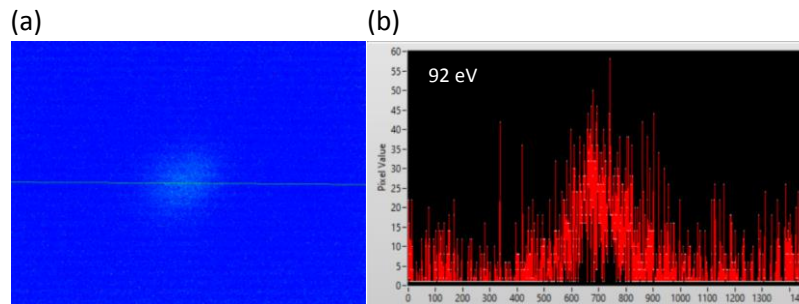


**Figure S10.** (a) Image and (b) intensity profile of 13.5 nm radiation, obtained with a fiber-coupled DEUVI system at its detection limit. The beam flux was  $3.9 \times 10^8$  photons/s, and the camera was operated at an exposure time of 1 s and a gain of 30 dB. The sensing area of the CMOS camera was  $4.97 \text{ mm} \times 3.73 \text{ mm}$ .